Journal of Hydro-environment Research 25 (2019) 1–11

Contents lists available at ScienceDirect

Journal of Hydro-environment Research

journal homepage: www.elsevier.com/locate/jher

Envelope curves for the specific discharge of extreme floods in Malaysia

Jazuri Abdullah[a], Nur Shazwani Muhammad[b,*], Siti Asiah Muhammad[b], Pierre Y. Julien[c]

[a] Faculty of Civil Engineering, Universiti Teknologi MARA, Shah Alam, Selangor, Malaysia
[b] Smart and Sustainable Township Research Centre (SUTRA), Faculty of Engineering and Built Environment, Universiti Kebangsaan Malaysia, Bangi, Selangor, Malaysia
[c] Department of Civil and Environmental Engineering, Colorado State University, Fort Collins, USA

ARTICLE INFO

Keywords:
Peak specific discharge
Maximum estimated discharge
Rainfall duration
Large watershed
Extreme rainfall events
Hydrological modelling
PMP

ABSTRACT

The relationship between peak specific discharge and watershed area is examined for large, rare and extreme floods in Malaysia using a distributed hydrological model. Envelope curves for specific discharge for these events and the uncertainty is quantified. The relationships between rainfall duration and intensity as a function of watershed size were also examined. As a result, three main regions were defined to estimate the peak discharge as a function of watershed size for large, extreme and rare floods. The average magnitudes for the PMP and the world's extreme rainfall events were 5 and 12 times larger than the 100-year event, respectively. The envelope curves may assist engineers and other interested parties to estimate the peak discharge for watershed up to 100,000 km^2, especially for ungauged watersheds.

1. Introduction

Generally, the frequency and magnitude of floods in Malaysia are very high. Malaysia is prone to flood risks, mostly by nature of its physical geography (e.g. topography and drainage) and human geography (e.g. settlement and land use). The monsoon climate usually brings floods between November and February. Historically, Malaysia experienced floods almost every year. However, the most devastating major floods of the 20th century were recorded in 1926, 1963, 1965, 1967, 1969, 1971, 1973, 1979, 1983, 1988, 1993, and 1998. For the past 20 years, the most memorable major floods occurred in December 2006/January 2007 (Johor), 2009/2010 (Kedah and Perlis) and 2014 (Kelantan, Terengganu and Pahang). The major floods in Kedah and Perlis in 2009/2010 covered two states of northern Peninsular Malaysia that are considered relatively dry. Deforestation and urbanization cause changes from pervious to impervious surfaces which increase the runoff discharge and flow velocity while significantly decreasing the time of concentration. The cost of damage for the flood events in 2010 increased by 800% when compared with the floods of 1982 (Chan, 2017).

The occurrence of natural disasters, as a result of extreme hydrological events has increased in recent years. Scientists and researchers are increasingly motivated to enhance their understanding of the increasing variability in climatic patterns. Currently, hydrologists use the concept of Annual Exceedance Probability (AEP) to describe the frequency of extreme hydrological events and also to quantify the risk of failure of engineering structures. Nathan and Weinmann (1999) categorized rainfall and flood events as large, rare and extreme, as shown in Fig. 1. Large events can be obtained from interpolation techniques with moderate uncertainty and range from one in fifty years to one in one hundred years of AEP. An extrapolation from the known to the unknown and a pragmatic approach based on theoretical upper limits were used to estimate rare and extreme events, respectively. Rare events do not exceed a 2000 years AEP, and extreme events exceed a 2000 year AEP. Additionally, the upper and lower limits of uncertainty increased from large to extreme events. Nathan and Weinmann (1999) also concluded that the rare and extreme events are beyond the credible limit of extrapolation. Therefore, observed data, especially during large, rare and extreme hydrological events are very important as they contain important information in terms of rainfall precipitation and watershed response, time to peak and peak discharge.

In many developing countries including Malaysia, limited data measurements are available during large floods with regard to rainfall precipitation and storm duration, flow discharge and water levels. Like many other countries, the scarcity of data prevails for extreme events due to equipment malfunction, inaccessibility to the affected areas and lack of technologically-advanced gauging equipment. Therefore, it becomes increasingly important to gather more information on the predicted rainfall-runoff relationships during rare and extreme floods. Information such as peak discharge and time to peak are needed to determine the water levels during floods and the corresponding inundation area.

Current practice on the estimation of peak discharge mainly

* Corresponding author.
E-mail address: shazwani.muhammad@ukm.edu.my (N.S. Muhammad).

https://doi.org/10.1016/j.jher.2019.05.002
Received 27 February 2018; Received in revised form 13 May 2019; Accepted 27 May 2019
Available online 28 May 2019

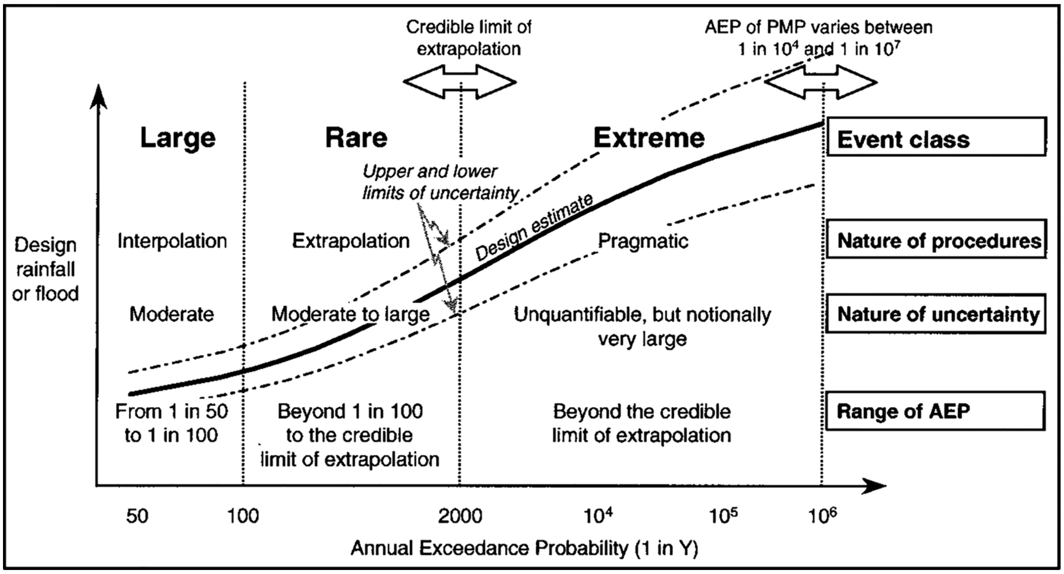

Fig. 1. Definition of large, rare and extreme rainfall / flood events (adapted from Nathan and Weinmann, 1999).

requires extensive physical and hydrological data. Although these methods are well developed and widely used in engineering practices, the values are normally site specific because it depends on many localized factors such as rainfall amounts and duration, channel length and slope, land use and drainage area (Dillow, 1998; Weaver, 2003; Zhang et al., 2001; Calenda et al., 2005; Tremblay et al., 2008; Bhatt and Tiwari, 2008; Grimaldi and Petroselli, 2015). Research on simplifying the relationship of peak discharge with temporal and spatial variability using power laws were reported by Furey and Gupta (2005), Furey and Gupta (2007), Ayalew et al. (2014) and Patnaik et al. (2015). Extensive observed streamflow and rainfall data were used to develop an equation for peak discharge estimation using multiple linear regression techniques. Therefore, the equations developed were seasonal and site specific and unsuitable outside the study area. Additionally, certain case studies show that the coefficient of determination R^2 is low and the relationship may not be reliable to estimate the peak discharge (Patnaik et al., 2015).

To overcome the need for extensive hydrological data and physical characteristics of a given watersheds, several researchers (Fill and Steiner, 2003; Taguas et al., 2008; Deng et al., 2016; and Chan, 2017) suggested a method to estimate instantaneous peak discharge using mean daily flow. These researchers used regression models to develop the relationship between the instantaneous peak discharges and mean daily flow. The applications of instantaneous peak discharge include the design flood flow for hydraulic structures and establishment of reservoir operation rules. The results assist engineers in estimating instantaneous peak discharge in an ungauged catchment because the relationship is regional. Although less extensive data is required, this method is unsuitable for locations where long and reliable streamflow data with good quality data is scarce.

On the other hand, traditional methods, such as Snyder unit hydrograph, Soil Conservation Service (SCS) and rational method estimate peak discharge using catchment characteristics such as land use, soil cover, and channel slope and geometry. A similar approach was adopted by El-Hames (2012) where he suggested a method to estimate peak discharge in ungauged arid and semi-arid areas using watershed characteristics. The method has been extensively calibrated and validated using data from six countries. Encouraging results are shown for catchment areas larger than 45 km^2. However, the result for small watersheds covering less than 45 km^2 is fair. Even though this method provides an alternative to estimate peak discharge where hydrological data is scarce, rigorous physical watershed characteristics are needed in order to perform the analysis. Other researchers using a similar method include: Suprit et al. (2010), Al-Rawas and Valeo (2010), and El-Hames and Al-Wagdany (2012). Estimates of the magnitude and frequency of flood-peak discharges are used for a variety of purposes, such as for the design of bridges, culverts, dams, and flood-control structures; and for the management and regulation of flood plains. To provide simple methods of estimating flood-peak discharges, most countries and states have developed and published general equations. These equations are produced from a large number of historical flood data, either for a specific region or at the global scale. Basically, two approaches are used for estimating the flood-peak discharges and these methods are based on: 1) the statistical analysis of data collected at gauging stations; and 2) the use of rainfall characteristics with a deterministic watershed model that uses equations and algorithms to convert rainfall excess to flood runoff (Jennings et al., 1994). These statistical equations are used to transfer flood characteristics from gauged to ungauged sites using watershed and climatic characteristics as explanatory or predictor variables. Generally, these equations have been developed on a regional area basis. The combination of these data has been widely used for over a century since Fuller (1914) to derive Envelope Curves (ECs) defined as the relationship between peak discharges and watershed area (e.g. Jarvis, 1925; Stedinger, 1993; Pilgrim and Cordery, 1993; Klemes, 1993). An envelope curve shows the relationship between the flood record of a gauge site and its catchment area in a log-log-diagram. This method has been applied worldwide at different scales: e.g. part of Greece (Mimikou, 1984), or Europe and the World (Herschy, 2002). The suggested ECs have been used for the comparison purposes for most of the watershed areas in Croatia (Biondic et al, 2007). Mimikou (1984) and Bayazit and Onoz (2004) plotted the historical maximum discharge as a function of watershed area. They produce rational equations for a specific site of their study area. The ECs were compared with the exceedance probability in terms of Flood Record and Probable Maximum Flood, as discussed by Vogel et al. (2007), Castellarin (2007), Castellarin et al. (2009) and Viglione et al. (2012), Eagleson (1972), Fiorentino and Iacobellis (2001), Sivapalan (2005), Gaume (2006), Merz and Blöschl (2008), Viglione and Blöschl (2009), Viglione and Blöschl (2009).

The developed ECs can predict peak discharges at certain probability levels for ungauged basins of the area and can be used in specific engineering applications. The peak specific-discharge is defined as the ratio of the maximum discharge divided by the watershed drainage area. The analyses of extensive discharge records may not be available at many sites, especially in developing countries. The term and a plot of peak specific-discharge were first introduced by Creager (1939). He used flood data in the USA for the years 1890, 1913, 1921, 1934 and 1939. He believed that the large floods would increase with time as longer periods of recorded data would become available. Creager et al. (1945) collected more data from the USA and some other countries from various sources. Gupta (2001) described Creager's method in his book. Other researchers that further examine the relationship between peak specific-discharge and watershed size are Julien (2018), Smith et al. (2005a,b, 2007) and Javier et al. (2007a,b). However, due to short time series and rare extreme events, the results of a flood frequency analysis are uncertain, especially for return periods of more than 100 years. The uncertainty for each of the events, i.e. large, rare and extreme event, is different. This uncertainty increased as the AEP increased from 50 years to more than 2000 years. AN uncertainty analysis was conducted to describe the entire set of possible discharges based on several combinations of upper, lower limits and calibrated/validated values. Empirical ECs are a traditional method to appraise the upper bound of flood events (e.g. Castellarin et al., 2005; Mimikou, 1984). The Saxonian envelope curve provides an upper bound for each gauging station, which can be integrated into a flood frequency analysis with extreme value distribution with 4-parameters (EV4) (Guse et al., 2007). By using this approach, the estimation of discharge for high return periods seems to be more realistic. There are several sources that contributed to the uncertainty of discharge, which includes the measurement error in rainfall and discharge and the estimation of hydrological and hydraulic parameters in the hydrologic model (e.g. Renard et al., 2009; Abdullah and Julien, 2014).

Numerous approaches for quantifying the uncertainty in hydrologic predictions have been proposed, including the Generalized Likelihood Uncertainty Estimation (GLUE) (Beven and Binley, 1992), stochastic approach (Montanari and Brath, 2004), Bayesian approaches (Feyen et al., 2007; Thiemann et al., 2001; Huard and Mailhot, 2008; Marshall et al., 2007; Wagener and Montanari, 2011), instrumental-variable methods (Young, 1998), Kalman filter algorithm (Deng et al., 2016; Habert et al., 2016), quantile regression and uncertainty estimation based on local error and clustering (UNEEC) (Dogulu et al., 2015).

The main objective of this study is to delineate the upper and lower limits of ECs for three different flood events, i.e. large (from 2- to 100-year return periods), rare (100- to 2000- year return periods) and extreme events (> 2000-year return periods) for various watershed sizes in Malaysia. Additionally, we examine the relationship between rainfall duration and intensity as a function of watershed size. A two-dimensional fully-distributed model was applied in this study. Three different sizes of watersheds in Malaysia were examined. Data from the Department of Irrigation and Drainage (DID) Malaysia were used for the model calibration and validation purposes. The uncertainty analysis approach suggested by Mishra (2009) was used to classify the upper and lower limit for different rainfall events as a function of watershed. Some reported flood events in Malaysia are used to support the resulting graph.

2. Watershed characteristics

In order to examine the impact of peak discharge for different sizes of watershed, three different watershed sizes are considered: small (Lui-68 km^2), medium (Semenyih - 236 km^2) and large (Kota Tinggi - 1635 km^2). The watershed sizes are categorized following the criteria given by Singh (1995). Lui (small) and Semenyih (medium) watersheds are located in the state of Selangor, while Kota Tinggi (large) watershed is located in Johor. The study areas are located in Peninsular Malaysia, as shown in Fig. 2. In general, the country's rainfall patterns are highly influenced by the Southwest (May to September) and Northeast (November to March) monsoons. November is the wettest month, while June and July are the driest months. On average, these watersheds receive an annual rainfall of about 2500 mm and the ambient temperature ranges between 21 °C and 32 °C throughout the year.

Lui (small) watershed is located north of the Semenyih watershed. Land surface elevations range from 80 to 1,200 m above sea level (asl). Most of the area is covered with mountains (about 87%) and the rest with valleys. The average normal depth of the main river for this small watershed range between 0.23 m and 0.99 m. The top width of the main channel is assumed constant at 16 m along the river with an average channel bed slope of 0.04. The maximum discharge in the main channel ranged from 0.74 to 17.17 m^3/s during the flows used for calibration.

The topography of the Semenyih (medium) watershed ranges from 1100 m asl at the upstream end to 40 m asl at the outlet of the watershed. The average terrain slope is about 45% ranging between 4% and 85%, with very steep mountains (about 68% of the total area is covered by mountains), overhanging flat and wide valleys. The average normal depth of the main river channel for Semenyih (medium) ranges between 0.8 m and 2.49 m. The large watershed is located in Kota Tinggi, a district of Johor. Mountains cover about 20% of the watershed, with an elevation higher than 600 m. The lowest elevation is 4 m at the downstream end of the watershed.

These three watersheds were selected because of their long and reliable flooding records and available data to perform the flood simulations, such as rainfall depth, streamflow, Digital Elevation Model (DEM), land use and soil type.

3. Methodology

3.1. Rainfall intensity and duration

Large events in this study are defined for rainfalls with return periods ranging from 2 to 100 years. Extreme rainfall events include both the Probable Maximum Precipitation (PMP) and the world's largest rainfall events. The polynomial approximation from the Malaysia Urban Stormwater Management Manual (MSMA, 2000), in Eq. 1 is used to calculate the rainfall intensity for large rainfall events.

$$\ln(I_t^R) = a + b\ln(t) + c[\ln(t)]^2 + d[\ln(t)]^3$$

where I_t^R is the average rainfall intensity (mm/hr) for a given duration t (in minutes) with R representing the Average Return Interval (ARI) (years), and the fitting parameters a, b, c, d function of the ARI (Table 1). The values of a, b, c, d obtained from MSMA (2000) were used to calculate the average rainfall intensity from Eq. 1. The rainfall intensity for extreme rainfall events (i.e. Small and Medium Probable Maximum Precipitation (SM-PMP) and the Large Probable Maximum Precipitation (L-PMP) were obtained from NAHRIM (2008) and Poon and Hwee (2010). Values from Jennings (1950) were used to simulate the world's largest rainfall events. The SM-PMP, L-PMP and world's event are listed in Table 2.

3.2. Hydraulic analyses using TREX

The use of numerical modeling in the estimation of peak discharge by simulating extreme events received considerable attention by researchers in the past few decades (Sangati et al., 2009; Abdullah et al., 2016; Khosronejad et al., 2016). This process-based method offers a different approach for estimating flood discharges. Typically, such models contain representations of surface runoff, sub-surface flow, evapotranspiration, and channel flow, but they can be far more complicated. The importance of these representations is useful to explain the existing situation and to simulate the future condition.

The hydraulic analyses in this study were carried out using the Two-dimensional Runoff Erosion and eXport (TREX) model (Velleux et al., 2006, 2008; England et al., 2007, 2014, 2018). Model state variables are water depth in the overland plane and stream channels. During calibration and validation processes, rainfall was distributed using IDW Kriging method in both time and space (Richardson et al., 1983; Ogden 1992; Ogden and Julien 1993, 1994, 2002; Jorgeson, 1999; Ogden

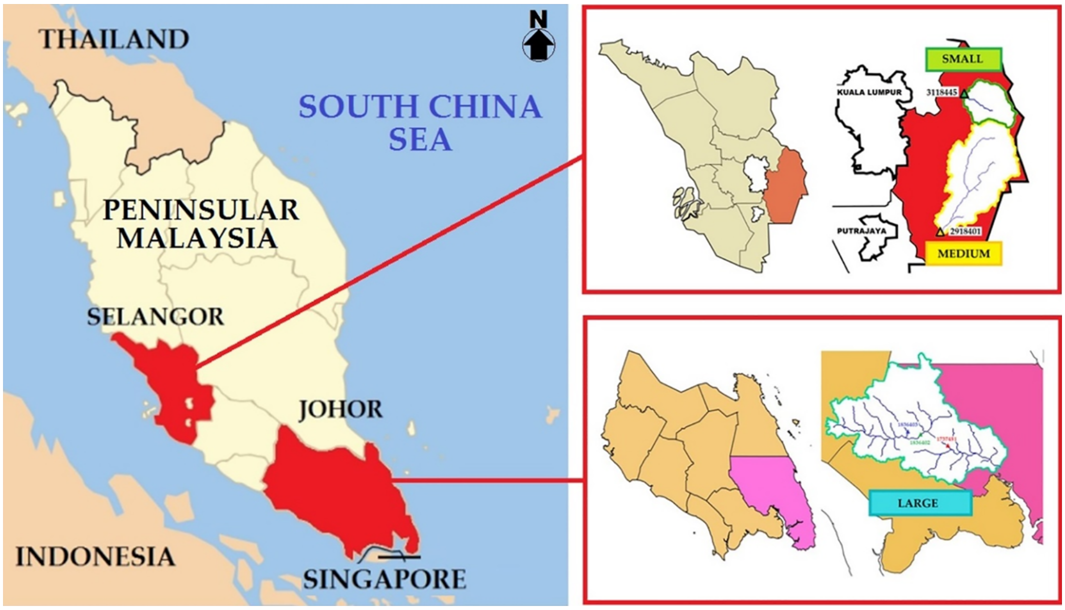

Fig. 2. Locations of small, medium and large watersheds on Malaysia's map (*Note: not to scale*).

et al., 2000). A uniform rainfall distribution was assigned for simulation of large, rare and extreme rainfall events. When spatially distributed precipitation is simulated, areal estimates are interpolated from point gage data using an inverse distance weighting approach. Interception and surface storage are simulated as equivalent depths. Infiltration and transmission loss rates are simulated using the Green and Ampt (1911) relationship. Overland and channel flows are simulated using the diffusive wave approximation in two- and one-dimensions, respectively. The explicit Euler method (Chapra and Canale, 1985) is used to compute the mass balances for each time step by counting all materials that enters, accumulates within or leaves a grid cell through precipitation excess, interception, infiltration, transmission losses and storage.

The calibration and validation processes, i.e. model performance in modeling the flood flow, are important in hydrological modeling. These processes were carried out using field measurements during several storm events. The performance of the model to find peak discharge, time to peak, and volume has been tested using three metrics: Relative Percentage Difference (RPD), Percentage Bias (PBIAS) and Nash-Sutcliffe Efficiency Coefficient (NSEC)) comparison. On average, the model performance was *good* for the small (RPD – 7%, PBIAS – 14% and NSEC – 0.4) and medium watersheds (RPD – 14%, PBIAS – 28% and NSEC – 0.7). The RPD (4%), PBIAS (2%) and NSEC (0.8) also demonstrate that the model performance was *very good* for the large watershed (Abdullah, 2013).

3.3. Uncertainty analysis of the peak specific-discharge

The uncertainty analysis for discharge was evaluated using only hydrological and hydraulic parameters. The hydrological and hydraulic

Table 2
Rainfall duration and intensity for SM-PMP, L-PMP and the world's largest events.

RAINFALL DURATION (hrs.)	SM-PMP (mm/hr)	L-PMP (mm/hr)	WORLD'S EVENT (mm/hr)
1	188	185.7	260.9
2	–	–	186.6
3	100	74.3	153.4
4	–	–	133.4
5	–	–	119.8
6	65.2	58.8	109.7
7	–	–	101.8
8	–	–	95.4
9	–	–	90.2
10	–	–	85.7
11	–	–	81.8
12	43.2	44.0	78.4
13	–	–	75.5
14	—	–	72.8
15	–	–	70.4
16	–	–	68.3
24 (1-day)	25.7	27.3	56.1
48 (2-days)	—	19.3	40.1
72 (3-days)	–	14.8	33.0
120 (5-days)	6.5	10.8	25.8
168 (7-days)	4.9	9.1	21.9

Note: PMP = Probable Maximum Precipitation; SM-PMP = Small-Medium PMP; L-PMP = Large PMP.

Table 1
Coefficients for the polynomial approximation of rainfall intensity for small and medium ($30 \le t \le 1000$ min) and large ($30 \le t \le 10080$ min) watersheds.

Average Recurrence Interval (Year)	SMALL & MEDIUM WATERSHEDS (LARGE WATERSHED)			
	a	b	c	d
2	4.2095 (5.1028)	0.5056 (0.2883)	−0.1551 (−0.1627)	0.0044 (0.0095)
5	5.1943 (5.7048)	− 0.0350 (−0.0635)	−0.0392 (−0.0771)	−0.0034 (0.0036)
10	5.5074 (5.8489	− 0.1637 (−0.0890)	−0.0116 (−0.0705)	−0.0053 (0.0032)
20	5.6772 (4.8420)	−0.1562 (0.7395)	−0.0229 (−0.2579)	−0.0040 (0.0165)
50	6.0934 (6.2257)	−0.3710 (−0.1499)	0.0239 (−0.0631)	−0.0073 (0.0032)
100	6.3094 (6.7796)	−0.4087 (−0.4104)	0.0229 (−0.0160)	−0.0068 (0.0005)

Table 3
Parameters bound for uncertainty analysis at small, medium and large watersheds: hydraulic conductivity and Manning's *n*.

PARAMETER	LOWER LIMIT	UPPER LIMIT	APPLICATION
SMALL WATERSHED			
Hydraulic Conductivity, K_h (m/s)	1.31×10^{-7}	3.405×10^{-7}	Sandy loams
	1.14×10^{-7}	3.930×10^{-7}	Loams
	4.34×10^{-7}	1.301×10^{-6}	Mountain - limestone
Manning's n	0.085	0.255	Agricultural
	0.025	0.075	Urban/ Commercial
	0.200	0.600	Forest
MEDIUM WATERSHED			
Hydraulic Conductivity, K_h (m/s)	5.60×10^{-9}	1.68×10^{-8}	Sandy loams
	6.35×10^{-9}	1.91×10^{-8}	Loams
	1.53×10^{-9}	4.59×10^{-9}	Clay
	5.90×10^{-11}	1.77×10^{-10}	Mountain - limestone
Manning's n	0.050	0.150	Agriculture
	0.025	0.075	Urban/ Commercial
	0.100	0.300	Forest
	0.050	0.200	Grass area
	0.050	0.150	Open area
LARGE WATERSHED			
Hydraulic Conductivity, K_h (m/s)	3.56×10^{-10}	1.07×10^{-9}	Sandy loams
	3.64×10^{-10}	1.09×10^{-9}	Loams
	3.59×10^{-11}	1.08×10^{-10}	Mountain - limestone
Manning's n	0.15	0.45	Agriculture
	0.01	0.03	Urban/ Commercial
	0.30	0.90	Forest
	0.15	0.45	Grass area
	0.15	0.45	Open area

parameters for TREX model include the hydraulic conductivity, K_h, soil moisture deficit, hydraulic suction head, H_c, slope (overland, S_{ov}, and channel, S_{ch}), roughness (Manning's *n* for overland, n_{ov}, and channel, n_{ch}). These parameters were known to be the most sensitive parameters as discussed by Abdullah and Julien (2014) and Abdullah et al. (2014). The K_h and Manning's *n* vary widely between soil classes and land covers, respectively. The variation of the Manning's *n* depends on the type and condition of vegetative cover. Upper and lower K_h and Manning's *n* values were assumed to be 50% larger and lower than the calibrated value. To simplify the analysis, only the variation of the overland roughness was explored.

The Logic Tree Analysis (LTA) approach as described by Mishra (2009) was used. The author suggests that this approach is particularly useful for uncertainty propagation when parameter uncertainty is described using a limited number of possibilities (e.g., upper and lower limit, and calibrated and validated parameters values). The LTA is ordered such that the sum of the possibilities is unity (i.e., 1.0) when the combination of upper and lower limits were used. The upper (UP) and lower limits (LL) were selected using the ± 50% of calibrated and validated values (Table 3). These limits were introduced to determine the uncertainty (possible range) of maximum estimated discharge (MED) for different rainfall events. It is known that any models are subjected to a range of uncertainties caused by several factors, such as model structure, input data and model process parameters. Through the sensitivity analysis conducted by Abdullah and Julien (2014), model process parameters in TREX model were known to be most sensitive. These parameters are the hydraulic conductivity, K_h, and Manning roughness, *n*. The uncertainty analysis was conducted to determine the upper (UP) and lower bound (LL). Data from Table 3 were used to estimate MED by using the combination of LL (K_h) and LL (n), LL (K_h) and UP (*n*), UP (K_h) and LL (*n*), UP (K_h) and LL (*n*), UP (K_h) and calibration/validation (CV), LL (K_h) and CV, UP (*n*) and CV and LL (*n*) and CV. These limits correspond to the maximum and minimum permissible values of hydrology and hydraulic parameters (will be referred to as the model parameters in the following paragraph) in hydrological model as suggested by Liong et al. (1989). The model parameters depend on the soil types and topography of the watersheds. The assumption is that these model parameters do not change much as compared to the land use, unless there is a significant work in replacing the existing soil type on the watershed area. The ± 50% limits were chosen to depict the plausible and realistic range of parameter uncertainty for the key inputs to assess variability in the system outputs.

4. Results and discussion

4.1. Model parameterization

The TREX model was used to simulate infiltration, overland runoff, and channel flow during extreme rainfall events. Input data were prepared using ArcGIS 9.3 and converted into text files. The watersheds were discretized at a 90 by 90 m grid size for small and medium watersheds, and a 230 by 230 m grid size for large watersheds. These grid sizes are selected based on the study conducted by Shrestha et al. (2002, 2006).

The model calibrations for the small and medium watersheds were done using recorded data at stations 3118445 and 2918401, respectively. For large watershed, three flow gauges (i.e. 1836403, 1836402 and 1737451) were used during calibration and validation processes. The calculated RPD, PBIAS and NSEC values are classified based on the criteria given in Table 4. Most of the peak discharge and time to peak values indicate that the model shows excellent performances specified by RPD and NSEC values of less than 10% and more than 0.7, respectively, except for a few events (Table 5).

4.2. Relationship between rainfall duration, peak specific-discharge and watershed area

The Maximum Estimated Discharges (MED) for large rainfall events were highest for rainfall durations of 3 to 5 hours on small watersheds. However, the MED values for medium watersheds were obtained for rainfall durations between 5 and 12 hours. The MED values for extreme rainfall events were highest for rainfall durations between 10 and 13 hours on both watersheds. For the large watershed, the MED values of large and extreme events corresponded to a rainfall duration of 168 hours.

Fig. 3 is a log-log graph that shows the relationship of the rainfall duration for highest maximum estimated discharge (MED) value estimated by the model for each large and extreme event as a function of watershed size. The highest MED value was selected and the rainfall duration for that particular event was determined. For instance, for a

Table 4
General performance ratings to classify the performance of the model.

PERFORMANCE RATING	RPD and PBIAS	NSEC
Very Good	RPD, PBIAS ≤ ± 10%	0.75 ≤ NSEC < 1.00
Good	± 10% < RPD, PBIAS ≤ ± 15%	0.65 ≤ NSEC < 0.75
Fair / Satisfactory	± 15% < RPD, PBIAS ≤ ± 25%	0.36 ≤ NSEC < 0.65

Table 5
Summary of the evaluation of hydrologic model performance for the small, medium and large watersheds.

WATERSHED SIZE		Date of Event MM/DD/YY	Peak flow (m^3/s)			Time to peak (24 h)			Model's performance	
			Obs.	Sim.	RPD (%)	Obs.	Sim.	RPD (%)	NSEC	PBIAS
SMALL	C	04/10/09	23.99	24.01	0.1	22:00	21:11	− 3.7	0.4	50.6
	V	10/20/09	16.60	17.00	2.4	22:00	20:35	−6.4	0.8	−11.4
		05/14/09	16.51	13.74	−16.8	07:00	07:18	4.2	0.8	−11.1
		01/03/09	14.67	13.37	−8.8	18:00	14:42	−18.3	0.7	−7.6
MEDIUM	C	04/13/03	39.98	40.15	0.4	20:00	20:18	1.5	0.8	−19.3
	V	04/03/08	77.58	77.77	0.2	23:00	23:54	3.9	1.0	−7.6
		11/10/02	27.71	27.74	0.1	00:00	00:42	41.0	0.8	−25.9
		10/01/04	43.12	43.18	0.1	19:00	19:21	1.8	0.8	−28.9
LARGE	C	11/11/10 – 12/04/10								
	Stn. 1836403		5.14	5.73	11.5	12:00	12:00	0.0	0.8	0.1
	Stn. 1836402		30.18	30.18	18.7	00:00	18:00	25.0	0.6	1.1
	Stn. 1737451		97.68	97.67	−1.0	12:00	12:00	0.0	1.0	−2.9
	V	05/07/10 – 05/17/10								
	Stn. 1836403		8.34	7.94	−4.8	06:00	06:00	0.0	0.9	5.9
	Stn. 1836402		28.56	27.56	−3.5	00:00	06:00	25.0	0.9	−12.1
	Stn. 1737451		51.36	48.96	−4.7	12:00	18:00	25.0	1.0	−1.2

Note: C = Calibration; V = Validation; Obs. = Observed; Sim. = Simulated; RPD = Relative Percentage Different; NSEC = Nash-Sutcliffe Efficiency Coefficient; PBIAS = Percent BIAS.

100-year return period event at the small watershed, the highest estimated MED value was 91 m^3/s for rainfall duration of 4 hours. For the large rainfall events (refer to Table 6), the duration of rainfall to reach the highest MED values for large rainfall events at small and medium watersheds vary. The rainfall duration between 3 and 5 hours was estimated by the model for the small watershed. For the medium watershed, the rainfall duration increased between 5 and 12 hours. However, for the large watershed, the rainfall duration were simulated for 7 days to reach the highest MED for all large rainfall events. Similar to a large event, the duration of rainfall for the model to estimate highest MED is not the same as at the small, medium and large watersheds. A sample from the TREX simulation events from Abdullah (2013) is presented in Fig. 4 showing the model calibration on the large watershed at Kota Tinggi. Similarly, Fig. 5 shows the TREX simulation of the world largest precipitation event on the medium size watershed at Semenyih. The TREX model estimated the MED values for small and medium watersheds with the duration of rainfall between 10 and 13 hours (refer to Fig. 3. – yellow and red dots). However, for the large watershed, the rainfall duration increased to 168 and 150 hours for the KT-PMP and world's largest rainfall events, respectively.

The topography of the small and medium watersheds is approximately similar, i.e., more than 50% of the watershed is mountainous, while more than 50% of the large watershed is a low land area. The topography difference between these watersheds affected the time to reach MED for each simulated event. For the large watershed, the low land area is covered by forest and some places are swampy. Generally,

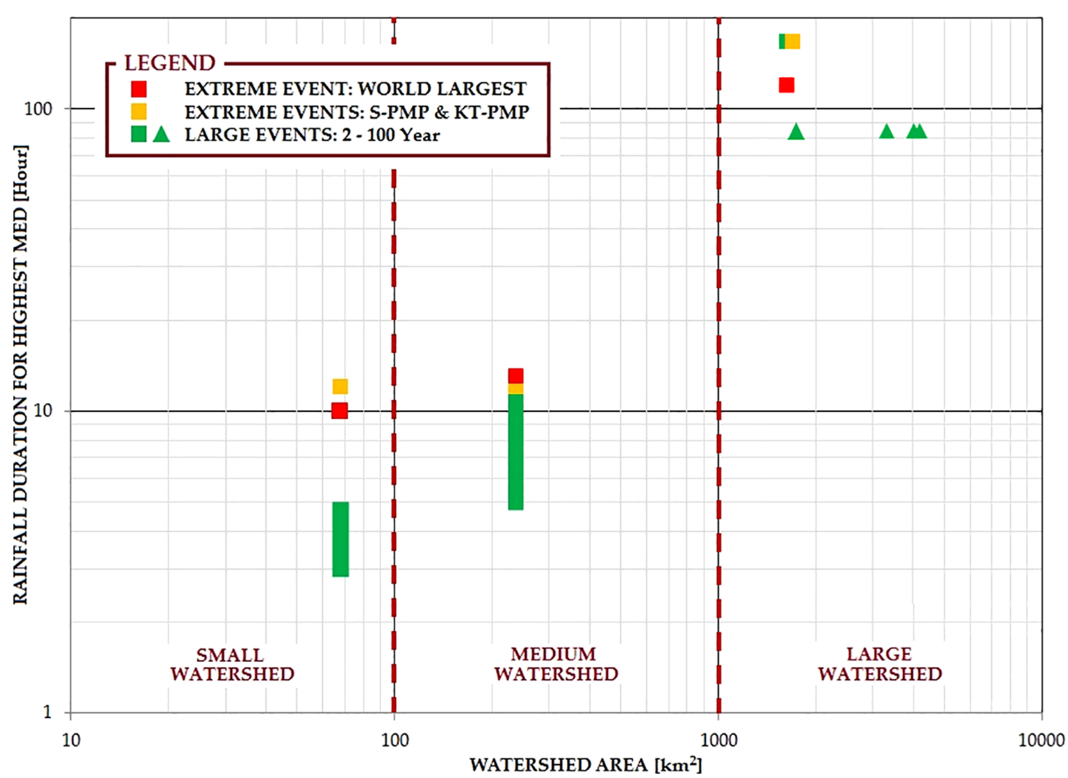

Fig. 3. The relationship between duration of rainfall of the highest MED value and the watershed area.

Table 6
Duration of rainfall contributed to highest MED value and peak specific-discharges.

Rainfall Events		Watershed size (in km^2)								
		Small (68)			Medium (236)			Large (1635)		
		Highest MED (m^3/s)	Rainfall Duration (hrs)/ Rainfall intensity (mm/hr)	Peak Specific-Discharge ($m^3/s/km^2$)	Highest MED (m^3/s)	Rainfall Duration (hrs)/ Rainfall intensity (mm/hr)	Peak Specific-Discharge ($m^3/s/km^2$)	Highest MED (m^3/s)	RainfallDuration (hrs)/Rainfall intensity (mm/hr)	Peak Specific-Discharge ($m^3/s/km^2$)
Large Events	2-year	22	3/26	0.32	147	5/18	0.62	368	168/4	0.23
	5-year	46	5/22	0.68	167	12/10	0.71	–	–	–
	10-year	62	5/25	0.91	206	5/25	0.87	–	–	–
	20-year	74	5/27	1.09	226	12/12	0.96	–	–	–
	50-year	85	4/36	1.25	242	12/14	1.03	920	168/7	0.56
	100-year	91	4/38	1.34	256	12/15	1.08	1023	168/8	0.63
Extreme Events	PMP	520	12/43	7.65	1474	12/43	6.25	3016	168/9	1.84
	World	1358	10/78	19.97	3793	13/77	16.07	8332	120/25	5.10

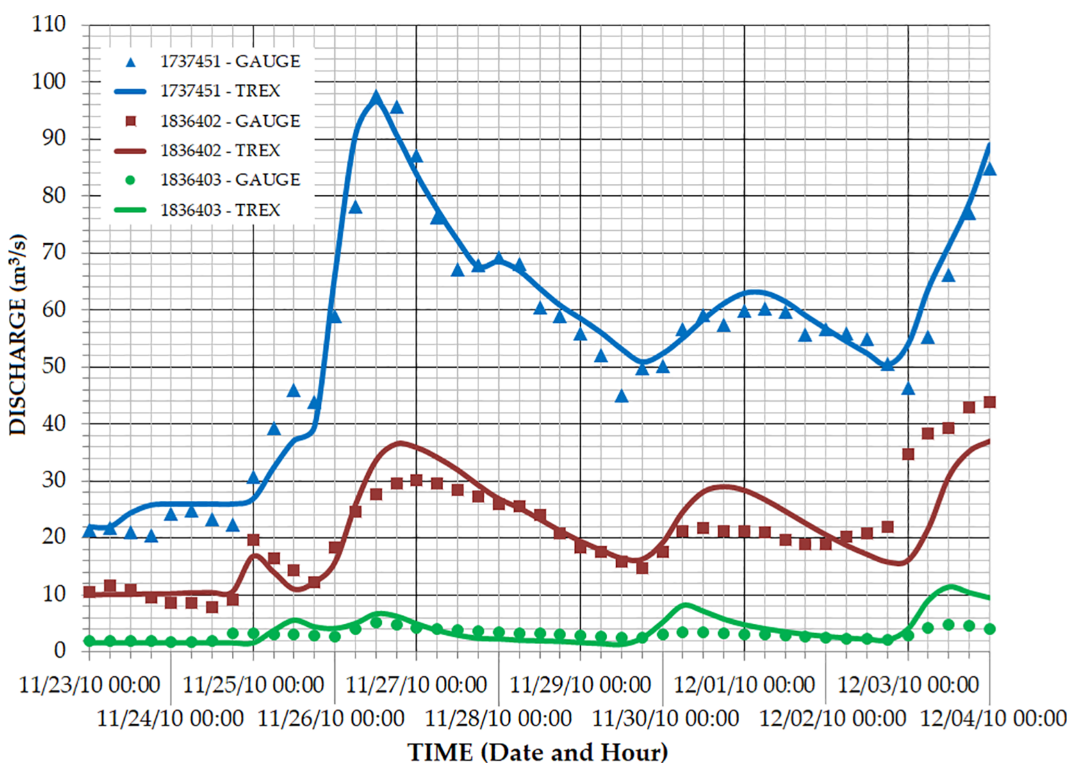

Fig. 4. Model calibration on large size (Kota Tinggi) watershed.

the tropical rain forest is dense with large trees, which increases the travel time down the watershed.

During extreme rainfall events, the intensity of rainfall is very high compared to large rainfall events. Therefore, the soils become fully saturated in a very short period of time. As a result, more overland flow was generated because the rainfall exceeded infiltration rates. Increasing rainfall intensity by a factor of 2.0 (for small and medium watersheds) and 1.6 (for large watershed) from the 100-year return period to PMP event and from PMP to the world's largest event creates rainfall beyond the normal conditions. It means that by increasing the intensity of rainfall, the discharge in the main channel and overland will be much different than during normal events. During normal events, the flow in the main channel is controlled by the channel itself. However, as the rainfall intensity and duration are far beyond the normal conditions, the flow conveyance and distribution is controlled by the rainfall event. The channel and overland surface roughness decrease as the flow depth and volume increase. As a result, the MED values are significantly increased.

The relationship between rainfall duration and intensity as a function of watershed size is interesting as well. The MED for the small and medium watersheds was obtained at rainfall durations between 3 and 13 hours (refer to Table 6). This means, the MED values are influenced by rainfall intensity, i.e. as the rainfall duration is increasing, the rainfall intensity is decreasing. However, for the large watershed, the duration of rainfall to obtain MED values are longer than the other two watersheds. Except for the world's largest event, the MED values are estimated at 168 hours of rainfall duration (Table 6). The MED value for the world's largest event is estimated when the duration of rainfall was 120 hours. To make this discussion easier, the rainfall duration of this event was assumed to be 168 hours, the same as other events for the large watershed, because the difference of MED values for 120 and 168 hours was less than 5%. Therefore, for the large watershed, the duration of rainfall is more important than the rainfall intensity in order to determine the MED value.

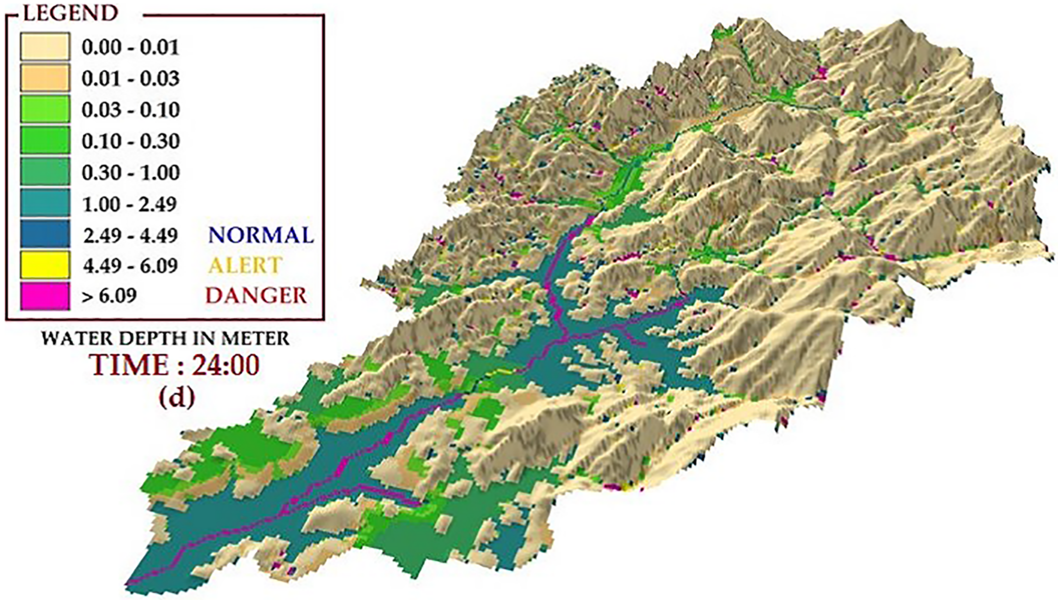

Fig. 5. Simulation of the world largest precipitation on the medium size (Semenyih) watershed.

Fig. 6 shows the relationship between the peak specific-discharge and watershed area. Also, the plotted values were calculated by dividing the highest MED for each specific event with the watershed area as tabulated in Table 7. The graph has been modified from Creager et al. (1945) and Julien (2018) in order to fit the results of this study. This graph was introduced by Creager et al. (1945) by plotting the highest floods observed from the USA and some big floods from other countries such as China, India and Brazil. Additional information, as shown in Table 7, was obtained from REDAC (2006) and UNESCO (1995, 1997, 2002, 2004), to support the findings from this study. REDAC (2006) estimate the peak discharges at four (4) different locations (refer to Table 7) and classified it for different large flood events (i.e. from 2- to 100-year ARI). These data were used to support the establishment of large flood events (i.e. green region of Fig. 6) in Malaysia. Data reported by UNESCO (1995, 1997, 2002, 2004) were used to establish the extreme region. Based on these reports, these values claimed to be most severe flood events in Malaysia. Therefore, from this information, three regions were established: large events covering return periods between two to 100-years, PMP, and world's largest rainfall event. These regions were classified using 50% lower and upper limits from the minimum

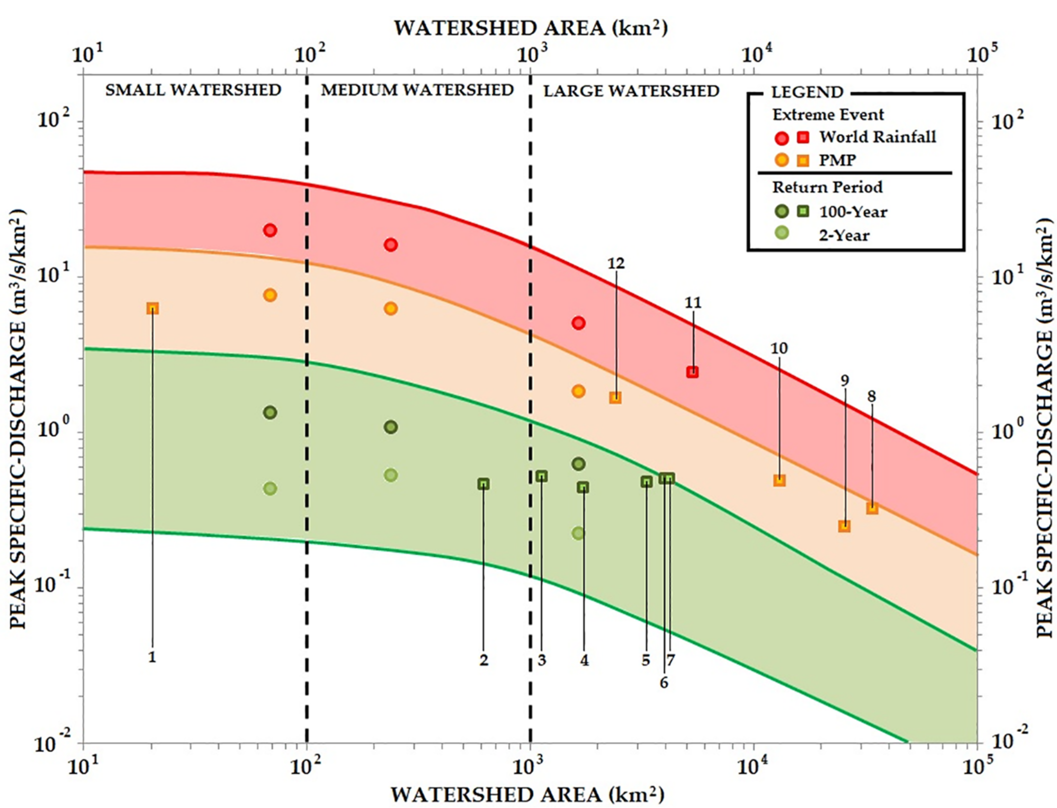

Fig. 6. Large and extreme peak specific-discharges as a function of watershed area with significant historical flood data in Malaysia.

Table 7
Peak specific-discharge data from other researchers.

Rainfall event	Highest MED (m^3/s)	Peak Specific-Discharge ($m^3/s.km^{-2}$)	Highest MED (m^3/s)	Peak Specific-Discharge ($m^3/s.km^{-2}$)	Highest MED (m^3/s)	Peak Specific-Discharge ($m^3/s.km^{-2}$)	Highest MED (m^3/s)	Peak Specific-Discharge ($m^3/s.km^{-2}$)
Station	Chalok Bridge [1] (Area = 20.5 km^2)		Sayong River [2] (Area = 624 km^2)		Johor River [3] (Area = 1130 km^2)		Kapit Wharf [8] (Area = 34,053 km^2)	
	127.7	6.23	288.7	0.46	587.9	0.52	10,799	0.32
Station	Jeniang [4] (Area = 1740 km^2)		Jambatan [5] (Area = 3330 km^2)		Ladang [6] (Area = 4010 km^2)		River Estuary [7] (Area = 4210 km^2)	
	667	0.38	1386	0.42	1768	0.44	1910	0.45
	767	0.44	1579	0.47	2000	0.50	2100	0.50
Station	Lubok Paku [9] (Area = 25,600 km^2)		Sg. Yap [10] (Area = 13,200 km^2)		Kuala Krai [11] (Area = 5387 km^2)		Kg. Tualang [12] (Area = 2480 km^2)	
	6318	0.25	6377	0.48	12,900	2.39	4020	1.65

Note: The source for [1],[11]&[12] are from UNESCO (2002); [2]&[3] are from UNESCO (1997); [4],[5],[6]&[7] are from REDAC (2006); [8] is from UNESCO (1995); [9]&[10] are from UNESCO (2004).

and maximum of the highest MED values in each region. The first region is represented in green. The region has a minimum limit to ensure that the design discharge is not under estimated. This is important so that any hydrologic design system, for example drainage or widening and deepening of a river could contain high discharge. The second region is represented in orange. The highest MED values resulted from S-PMP (small and medium watersheds) and KT-PMP (large watershed) events were used as benchmarks to produce this region. The outline of this region was produced using results from this study and supported by plotting the additional data as in Table 7, except for Fontaine (1992), which is plotted in large event region. Finally, the world's largest event, which is classified as extreme event, is presented in red. According to Nathan and Weinmann (1999), this event has the annual exceedance probability of at least 1 in 2000 years (Fig. 1). The upper bound is introduced to limit the design discharge. If the design discharge is beyond this region, the results certainly should be double checked because they are highly improbable.

The variability of the peak specific discharge decreases for the extreme events (i.e., PMP and world's largest rainfall events). At this point, the hydrologic parameters do not play any role because the soils become fully saturated and the roughness is small. The coverage for all regions decreases as size of watershed increases. The peak specific-discharge decreased trivially as the watershed size increased up to 1×10^3 km^2. For one log-cycle of watershed size, the peak specific-discharge decreased about one-third log-cycle. However, beyond this watershed size (1×10^3 km^2), the value of peak specific-discharge is decreased significantly. The peak specific-discharge decreased more than a half log-cycle. The distributions of these regions are related to the magnitude (or ratio), as shown in Table 8. As shown in Table 8, the magnitude (or ratio) of the highest MED values for the extreme events to the large event (100-year return period) is about the same. The average magnitude is 5 and 12 times bigger for the respective events.

4.3. The uncertainty of the peak specific-discharge

Fig. 7 shows the uncertainty value of the peak specific-discharge as a function of watershed area. The UP and LL were obtained from sensitivity analysis as discussed earlier. The uncertainty of the 100-year flood at small watershed is ± 20% from the estimation of calibrated/validated value; while medium and large watersheds give ± 10% for the same comparison. However, the uncertainty of peak discharges for PMP event shows increasing bounds (i.e., lower and upper limit) at small and medium watersheds. The values are ± 30% and ± 22%, respectively. The uncertainty of the peak discharge at large watershed for PMP event is ± 8%. For the world's largest rainfall event, the uncertainty of the peak discharge at small, medium and large watersheds is ± 16%. As the annual exceedance probability (AEP) increase (i.e. 1 in Y year), the uncertainty value is increasing, especially from large events to extreme events (i.e. PMP). For the world's largest rainfall event, the uncertainty is approximately same for all watersheds. This study indicated that for this event, the characteristics of the watershed do not contribute to the peak discharge anymore. The peak discharges were primarily influenced by the duration of rainfall. This can be seen through Fig. 7 – red region. The bell distribution which represent nine (9) possible peak discharges which were simulated using TREX model using LTA approach by Mishra (2009), as discussed in Section 3.3. The distribution of large, PMP and world's largest event, as shown in Fig. 6 is classified by considering the data reported by Creager et al. (1945) (for world historical flood events) and Malaysia data, which were obtained from REDAC (2006) and UNESCO (1995, 1997, 2002, 2004).

Table 8
Highest MED values for 100-year, PMP and World event.

WATERSHED SIZE	MAXIMUM DISCHARGE, Q_p (m^3/s)				
	100-year	PMP	Ratio [PMP/ 100-year]	World	Ratio [World/ 100-year]
SMALL (68 km^2)	91	520	6	1358	15
MEDIUM (236 km^2)	256	1474	6	3793	15
LARGE (1635 km^2)	1023	3016	3	8332	8

5. Summary and conclusions

From this study, the simulations of large and extreme events on small, medium and large watersheds in Malaysia using the TREX model demonstrate the following:

(a) The intensity of rainfall is the main factor in determining the flood magnitude of small and medium watersheds. The flooding events of large watersheds resulted from longer rainfall durations.
(b) The highest Maximum Estimated Discharge (MED) values for each large event were obtained between 3 and 5 hours of rainfall duration for the small watershed, and between 5 and 12 hours on the medium watershed. The highest MED values for extreme rainfall events were estimated at rainfall duration between 10 and 12 hours for both watersheds. The large watershed required more time to reach the highest MED value for all events, which was 168 hours (7 days).
(c) The average magnitude for the PMP and the world's extreme rainfall events was 5 and 12 times bigger than the 100-year event, respectively.
(d) The graph showing the relationship between peak specific discharges and watershed areas was plotted (Fig. 6). From this graph, three main regions were produced to estimate the peak discharge for the three sizes of watersheds. These regions were established based on the rainfall events of large, PMP, and the world's largest rainfall events. The peak specific-discharge decreased slightly as the watershed size increased up to 1×10^3 km^2. However, beyond this watershed size, the value of peak specific-discharge decreased

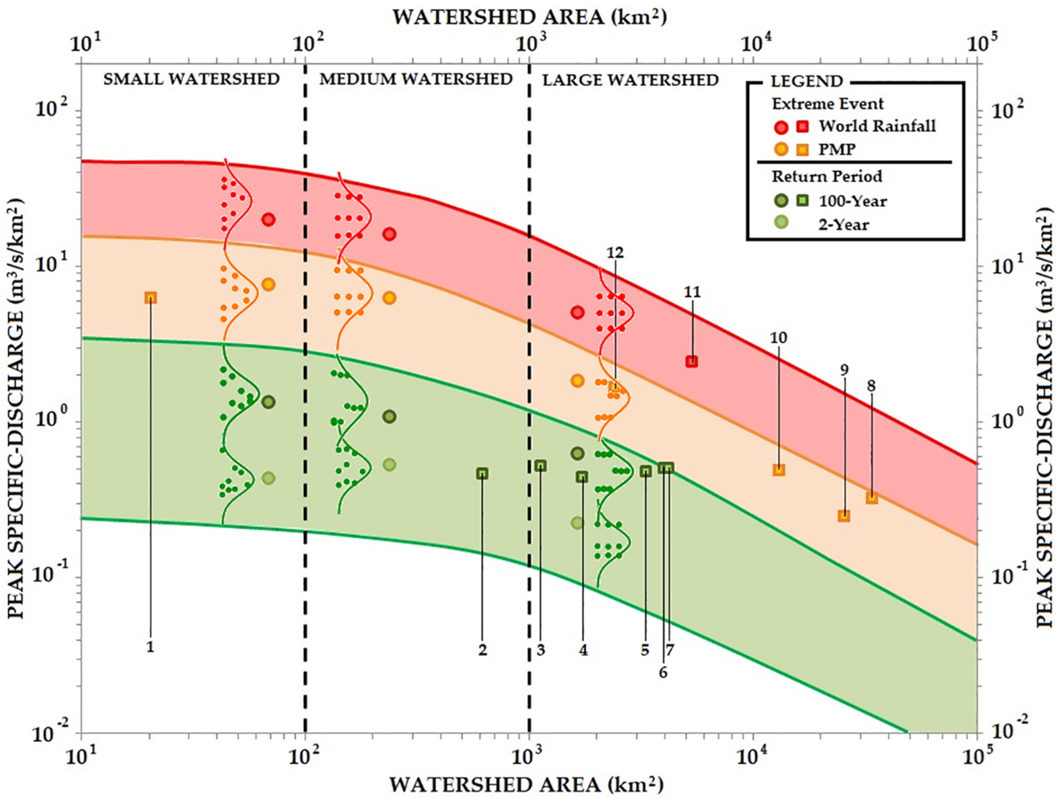

Fig. 7. Uncertainty of the peak specific-discharge as a function of watershed area.

significantly. The graph provides first-order approximations of the peak discharge and this approach can be particularly useful for the analysis of ungauged watersheds.

Acknowledgements

This study has been carried out at Colorado State University during the PhD studies of the first two authors. Financial support for the first and second author from the Ministry of Education, Malaysia, Universiti Teknologi MARA, Malaysia and Universiti Kebangsaan Malaysia is gratefully acknowledged. This work is also supported by additional funding from Universiti Kebangsaan Malaysia through Geran Penyelidikan Muda (GGPM-2014-046).

Declaration of Competing Interest

The authors declare no conflict of interest.

References

Abdullah, J., 2013. Distributed Runoff Simulation of Extreme Monsoon Rainstorms in Malaysia using TREX. Ph.D. Dissertation. Department of Civil and Environmental Engineering, Colorado State University, Colorado.
Abdullah, J., Julien, P.Y., 2014. Distributed flood simulations on a small tropical watershed with the TREX model. J. Flood Eng. 5, 17–37.
Abdullah, J., Kim, J., Julien, P.Y., 2014. Hydrologic modeling of extreme events. Encyclopedia Natural Resour.
Abdullah, J., Muhammad, N.S., Julien, P.Y., Ariffin, J., Shafie, A., 2016. Flood flow simulations and return period calculation for the Kota Tinggi Watershed, Malaysia. J. Flood Risk Manage.
Al-Rawas, G.A., Valeo, C., 2010. Relationship between wadi drainage characteristics and peak-flood flows in arid northern Oman. J. Sci. Hydrol. 55, 377–393.
Ayalew, T.B., Krajewski, W.F., Mantilla, R., Small, S.J., 2014. Exploring the effects of hillslope-channel link dynamics and excess rainfall properties on the scaling structure of peak-discharge. Adv. Water Resour. 64, 9–20.
Bayazit, M., Onoz, B., 2004. Envelope curves for maximum floods in Turkey. Teknik Dergi 15, 3125–3130.
Beven, K., Binley, A., 1992. The future of distributed models: model calibration and uncertainty prediction. Hydrol. Process. 6, 279–298.
Bhatt, V., Tiwari, A., 2008. Estimation of peak streamflows through channel geometry. J. Sci. Hydrol. 53, 401–408.
Biondic, D., Barbalic, D., Petras, J., 2007. Creager and Francou-Rodier envelope curves for extreme floods in the Danube River basin in Croatia, Predictions in Ungauged Basins: PUB Kick off (Proceedings of the PUB Kick-off meeting held in Brasilia, 20–22 November 2002). IAHS Publ, pp. 309.
Calenda, G., Mancini, C., Volpi, E., 2005. Distribution of the extreme peak floods of the Tiber River from the XV century. Adv. Water Resour. 28, 615–625.
Castellarin, A., 2007. Probabilistic envelope curves for design flood estimation at ungauged sites. Water Resour. Res, 43.
Castellarin, A., Vogel, R.M., Matalas, N.C., 2005. Probabilistic behavior of a regional envelope curve. Water Resour. Res, 41.
Castellarin, A., Merz, R., Bloschl, G., 2009. Probabilistic envelope curves for extreme rainfall events. J. Hydrol. 378, 263–271.
Chan, N.W., 2017. Challenges in Flood Disasters Management in Malaysia. IWRA Congress.
Chapra, S.C., Canale, R.P., 1985. Numerical Methods for Engineers with Personal Computer Applications, first ed. McGraw-Hill Inc., New York.
Creager, W.P., 1939. Possible and probable futures flood. Civ. Eng., New York 9, 668–670.
Creager, W.P., Justin, J.D., Hinds, J., 1945. Engineering for Dams: Volume 1 – General Design. John Wiley and Sons, New York.
Deng, C., Liu, P., Guo, S., Li, Z., Wang, D., 2016. Identification of hydrological model parameter variation using ensemble Kalman filterHydrol. Earth Syst. Sci. 20, 4949.
Dillow, J. J., 1998. Technique for simulating peak-flow hydrographs in Maryland.
Dogulu, N., López, P.L., Solomatine, D., Weerts, A., Shrestha, D., 2015. Estimation of predictive hydrologic uncertainty using the quantile regression and UNEEC methods and their comparison on contrasting catchments. Hydrol. Earth Syst. Sci. 19.
Eagleson, P.S., 1972. Dynamics of flood frequency. Water Resour. Res. 8, 878–898.
El-Hames, A., 2012. An empirical method for peak discharge prediction in ungauged arid and semi-arid region catchments based on morphological parameters and SCS curve number. J. Hydrol. 456, 94–100.
El-Hames, A., Al-Wagdany, A., 2012. Reconstruction of flood characteristics in urbanized arid regions: case study of the flood of 25 November 2009 in Jeddah, Saudi Arabia. J. Sci. Hydrol. 57, 507–516.
England, J.F., Julien, P.Y., Velleux, M.L., 2014. Physically-based extreme flood frequency analysis using stochastic storm transposition and paleoflood data. J. Hydrol. 510, 228–245.
England Jr., J.F., Cohn, T.A., Faber, B.A., Stedinger, J.R., Thomas Jr., W.O., Veilleux, A.G., Kiang, J.E., Mason Jr., R.R., 2018. In: Guidelines for Determining Flood Flow Frequency—Bulletin 17C: U.S. Geological Survey Techniques and Methods, book 4, chap. B5, pp. 148. https://doi.org/10.3133/tm4B5.
England, J., Velleux, M., Julien, P., 2007. Two-dimensional simulations of extreme floods on a large watershed. J. Hydrol. 347 (1), 229–241.
Feyen, L., Vrugt, J.A., Nualláin, B.Ó., van der Knijff, J., De Roo, A., 2007. Parameter

optimisation and uncertainty assessment for large-scale streamflow simulation with the LISFLOOD model. J. Hydrol. 332, 276–289.
Fill, H.D., Steiner, A.A., 2003. Estimating instantaneous peak flow from mean daily flow data. J. Hydraul. Eng. 8, 365–369.
Fiorentino, M., Iacobellis, V., 2001. New insights about the climatic and geologic control on the probability distribution of floods. Water Resour. Res. 37, 721–730.
Fontaine, T.A., 1992. Rainfall-runoff model accuracy for an extreme flood. J. Hydraul. Eng. 12, 365–437.
Fuller, W.E., 1914. Flood flows. Trans. Am. Soc. Civ. Eng. 77, 564–617.
Furey, P.R., Gupta, V.K., 2005. Effects of excess rainfall on the temporal variability of observed peak-discharge power laws. Adv. Water Resour. 2, 1240–1253.
Furey, P.R., Gupta, V.K., 2007. Diagnosing peak-discharge power laws observed in rainfall–runoff events in Goodwin Creek experimental watershed. Adv. Water Resour. 30, 2387–2399.
Gaume, E., 2006. On the asymptotic behavior of flood peak distributions. Hydrol. Earth Syst. Sci. 10, 233–243.
Green, W.H., Ampt, G.A., 1911. Studies on soil physics, 1: the flow of air and water through soils. J. Agric. Sci. 4, 11–24.
Grimaldi, S., Petroselli, A., 2015. Do we still need the rational formula? An alternative empirical procedure for peak discharge estimation in small and ungauged basins. Hydrol. Sci. J. 60, 67–77.
Gupta, S.G., 2001. Hydrology and Hydraulic Systems, second ed. Waveland Press.
Guse, B., Thieken, A., Merz, B., 2007. Estimation of upper bounds using envelope curves. Disaster Reduction Clim. Change 15.
Habert, J., Ricci, S., Le Pape, E., Thual, O., Piacentini, A., Goutal, N., Rochoux, M., 2016. Reduction of the uncertainties in the water level-discharge relation of a 1D hydraulic model in the context of operational flood forecasting. J. Hydrol. 532, 52–64.
Herschy, R.W., 2002. The world's maximum observed floods. Flow Meas. Instrum. 13, 231–235.
Huard, D., Mailhot, A., 2008. Calibration of hydrological model GR2M using Bayesian uncertainty analysis. Water Resour. Res. 44.
Jarvis, C., 1925. Flood flow characteristics. Paper Presented at the Proceedings of the American Society of Civil Engineers.
Javier, J.R.N., Smith, J.A., England, J., Baeck, M.L., Steiner, M., Ntelekos, A.A., 2007a. Climatology of extreme rainfall and flooding from orographic thunderstorm systems in the upper Arkansas River Basin. Water Resour. Res. 43, 1–13.
Javier, J.R.N., Smith, J.A., Meierdiercks, K.L., Baeck, M.L., Miller, A.J., 2007b. Flash flood forecasting for small urban watersheds in the Baltimore Metropolitan region. Bull. Am. Meteorol. Soc. 22, 1331–1344.
Jennings, A.H., 1950. In: World's Greatest Observed Point Rainfalls. Hydrometeorological Section. U. S. Weather Bureau, Washington D. C., pp. 4–5.
Jennings, M.E., Thomas, W.O., Riggs, H., 1994. Nationwide Summary of US Geological Survey Regional Regression Equations for Estimating Magnitude and Frequency of Floods for Ungaged Sites, 1993. US Geological Survey.
Jorgeson, J.J., 1999. Peak Flow Analysis Using A Two-dimensional Watershed Model with Radar Precipitation Data. Ph.D. Dissertation. Department of Civil and Environmental Engineering, Colorado State University, Fort Collins, Colorado.
Julien, P.Y., 2018. River Mechanics, second ed. Cambridge University Press, Cambridge, United Kingdom.
Khosronejad, A., Le, T., DeWall, P., Bartelt, N., Woldeamlak, S., Yang, X., Sotiropoulos, F., 2016. High-fidelity numerical modeling of the Upper Mississippi River under extreme flood condition. Adv. Water Resour. 98, 97–113.
Klemes, V., 1993. Probability of extreme hydrometeorological events—A different approach. In: Kundzewicz, Z. (Ed.), Extreme Hydrological Events: Precipitation, Floods and Droughts. Yokohama, Japan, IAHS, pp. 167–176.
Liong, S.Y., Selvalingam, S., Brady, D.K., 1989. Roughness values for overland flow in subcatchments. J. Irrig. Drain. Eng. 115, 203–214.
Marshall, L., Nott, D., Sharma, A., 2007. Towards dynamic catchment modelling: a Bayesian hierarchical mixtures of experts framework. Hydrol. Process. 21, 847–861.
Merz, R., Blöschl, G., 2008. Flood frequency hydrology: 1. Temporal, spatial, and causal expansion of information. Water Resour. Res, 44.
Mimikou, M., 1984. Envelope curves for extreme flood events in northwestern and western Greece. J. Hydrol. 67, 55–66.
Mishra, S., 2009. Uncertainty and sensitivity analysis techniques for hydrologic modeling. J. Hydroinfo 11, 282–296.
Montanari, A., Brath, A., 2004. A stochastic approach for assessing the uncertainty of rainfall-runoff simulations. Water Resour. Res, 40.
MSMA, 2000. Urban Stormwater Management Manual (MSMA Manual). Jabatan Pengairan dan Saliran Malaysia. DID – Department of Irrigation and Drainage, Malaysia 13-3.
NAHRIM, 2008. Technical guideline for estimating probable maximum precipitation for design floods in Malaysia. NAHRIM Technical Research Publication No. 1.
Nathan, R.J., Weinmann, P.E., 1999. Estimation of Large to Extreme Floods: Book VI in Australian Rainfall and Runoff, A Guide to Flood Estimation. The Institution of Engineers, Australia.
Ogden, F.L., 1992. Two-dimensional Runoff Modeling with Weather Radar Data. Ph.D. Dissertation. Department of Civil and Environmental Engineering, Colorado State University, Fort Collins, Colorado.
Ogden, F.L., Julien, P.Y., 1993. Runoff sensitivity to temporal and spatial rainfall variability at runoff plane and small basin scales. Water Resour. Res. 29, 2589–2597.
Ogden, F.L., Julien, P.Y., 1994. Runoff model sensitivity to radar rainfall resolution. J. Hydrol. 158, 1–18.
Ogden, F.L., Julien, P.Y., 2002. CHAPTER 4: CASC2D: a two-dimensional, physically-based, Hortonian hydrologic model. In: Singh, V.P., Frevert, D. (Eds.), Mathematical Models of Small Watershed Hydrology and Applications. Water Resources Publications, Littleton, CO, pp. 69–112.
Ogden, F.L., Sharif, H.O., Senarath, S.U.S., Smith, J.A., Baeck, M.L., Richardson, J.R., 2000. Hydrologic analysis of the Fort Collins, Colorado, flash flood of 1997. J. Hydrol. 228, 82–100.
Patnaik, S., Biswal, B., Kumar, D.N., Sivakumar, B., 2015. Effect of catchment characteristics on the relationship between past discharge and the power law recession coefficient. J. Hydrol. 528, 321–328.
Pilgrim, D. H., Cordery, I., 1993. Flood runoff. Handbook of hydrology, 9, 1–42.
Poon, H.C., Hwee, H.H., 2010. Probable maximum precipitation derivation in Malaysia: review and comparison. Int. J. Hydrol. Clim. Eng. 37–73.
REDAC, 2006. Design option of the flood mitigation plan of Sg. Muda, Sungai Muda, Kedah. Report, REDAC-USM.
Renard, B., Kavetski, D., Thyer, M., Kuczera, G., Franks, S., 2009. Understanding Predictive Uncertainty in Hydrologic Modeling: The Challenge of Identifying Input and Structural Errors. Water Resour. Res. American Geophysical Union, pp. 78.
Richardson, W.L., Smith, V.E., Wethington, R., 1983. Dynamic mass balance of PCB and suspended solids in Saginaw Bay – a case study. Physical behavior of PCBs in the Great Lakes. Ann Arbor Science Publishers, Ann Arbor, Michigan.
Sangati, M., Borga, M., Rabuffetti, D., Bechini, R., 2009. Influence of rainfall and soil properties spatial aggregation on extreme flash flood response modelling: an evaluation based on the Sesia river basin, North Western Italy. Adv. Water Resour. 32, 1090–1106.
Shrestha, R., Tachikawa, Y., Takara, K., 2002. Effect of forcing data resolution in river discharge simulation. J. Hydraul. Eng. 46, 139–144.
Shrestha, R., Tachikawa, Y., Takara, K., 2006. Input data resolution analysis for distributed hydrological modeling. J. Hydrol. 319, 36–50.
Singh, V. P., 1995. Computer models of watershed hydrology.
Sivapalan, M., 2005. Pattern, process and function: elements of a unified theory of hydrology at the catchment scale. Encyclopedia Hydrol. Sci.
Smith, J.A., Baeck, M.L., Meierdiercks, K.L., Nelson, P.A., Miller, A.J., Holland, E.J., 2005a. Field studies of the storm event hydrologic response in an urbanizing watershed. Water Resour. Res. 41, 1–15.
Smith, J.A., Miller, A.J., Baeck, M.L., Nelson, P.A., Fisher, G.T., Meierdiercks, K.L., 2005b. Extraordinary flood response of a small urban watershed to short-duration convective rainfall. Bull. Am. Meteorol. Soc. 6, 599–617.
Smith, J.A., Baeck, M.L., Meierdiercks, K.L., Miller, A.J., Krajewski, W.F., 2007. Radar rainfall estimation for flash flood forecasting in small urban watersheds. Adv. Water Resour. 30, 2087–2097.
Stedinger, J.R., 1993. Frequency analysis of extreme events. Handbook of Hydrology.
Suprit, K., Kalla, A., Vijith, V., 2010. A GRASS-GIS-Based Methodology for Flash Flood.
Taguas, E., Ayuso, J., Pena, A., Yuan, Y., Sanchez, M., Giraldez, J., Perez, R., 2008. Testing the relationship between instantaneous peak flow and mean daily flow in a Mediterranean Area Southeast Spain. Catena 75, 129–137.
Thiemann, M., Trosset, M., Gupta, H., Sorooshian, S., 2001. Bayesian recursive parameter estimation for hydrologic models. Water Resour. Res. 37, 2521–2535.
Tremblay, Y., Rousseau, A.N., Plamondon, A.P., Lévesque, D., Jutras, S., 2008. Rainfall peak flow response to clearcutting 50% of three small watersheds in a boreal forest, Montmorency Forest, Québec. J. Hydrol. 352, 67–76.
UNESCO-IHP (1995), Catalogue of rivers for Southeast Asia and the Pacific – Vol. Tachikawa, Y., James, R., Abdullah, K., Desa, M. N. M, (Eds.) Japan.
UNESCO-IHP (1997), Catalogue of rivers for Southeast Asia and the Pacific – Vol. Tachikawa, Y., James, R., Abdullah, K. and Desa, M. N. M, (Eds.) Japan.
UNESCO-IHP (2002), Catalogue of rivers for Southeast Asia and the Pacific – Vol. Tachikawa, Y., James, R., Abdullah, K. and Desa, M. N. M, (Eds.) Japan.
UNESCO-IHP (2004), Catalogue of rivers for Southeast Asia and the Pacific – Vol. Tachikawa, Y., James, R., Abdullah, K. and Desa, M. N. M, (Eds.) Japan.
Velleux, M., Julien, P.Y., Rojas-Sanchez, R., Clements, W., England, J., 2006. Simulation of metals transport and toxicity at a mine-impacted watershed: California Gulch Colorado. Environ. Sci. Technol. 40 (22), 6996–7004.
Velleux, M., England, J., Julien, P., 2008. TREX: spatially distributed model to assess watershed contaminant transport and fate. Sci. Total Environ. 404 (1), 113–128.
Viglione, A., Blöschl, G., 2009. On the role of storm duration in the mapping of rainfall to flood return periods. Hydrol. Earth Syst. Sci. 13 (2), 205–216. https://doi.org/10.5194/hess-13-205-2009.
Viglione, A., Castellarin, A., Rogger, M., Merz, R., Bloschl, G., 2012. Extreme rainstorms: comparing regional envelope curves to stochastically generated events. Water Resour. Res. 48.
Vogel, R.M., Matalas, N.C., England, J.F., Castellarin, A., 2007. An assessment of exceedance probabilities of envelope curves. Water Resour. Res. 43, W07403. https://doi.org/10.1029/2006WR005586.
Wagener, T., Montanari, A., 2011. Convergence of approaches toward reducing uncertainty in predictions in ungauged basins. Water Resour. Res. 47.
Weaver, J.C., 2003. Methods for estimating peak discharges and unit hydrographs for streams in the city of Charlotte and Mecklenburg County, North Carolina. US Department of Interior, US Geological Survey.
Young, P., 1998. Data-based mechanistic modelling of environmental, ecological, economic and engineering systems. Environ. Model. Softw. 13, 105–122.
Zhang, Y., Smith, J.A., Baeck, M.L., 2001. The hydrology and hydrometeorology of extreme floods in the Great Plains of eastern Nebraska. Adv. Water Resour. 24, 1037–1049.